

## Affinity characterization of monoclonal and recombinant antibodies for multianalyte detection with an optical transducer

Jacob Piehler <sup>a,\*</sup>, Andreas Brecht <sup>a</sup>, Thomas Giersch <sup>b</sup>, Karl Kramer <sup>b</sup>, Bertold Hock <sup>b</sup>,  
Günter Gauglitz <sup>a</sup>

<sup>a</sup> Universität Tübingen, Institut für Physikalische und Theoretische Chemie, Auf der Morgenstelle 8, D-72076 Tübingen, Germany

<sup>b</sup> Technische Universität München, Lehrstuhl für Botanik, Weihenstephan, D-85350 Freising, Germany

### Abstract

The selectivity of immunoassay is limited by the cross-reactivity of antibodies to structurally related analytes. This becomes a drawback for applications that require discrimination of slightly different analytes. An approach to overcoming this problem is the application of antibody arrays that show differences in their affinity patterns. We have investigated this method using systematic modelling of multianalyte systems based on test-independent affinity parameters. A model system of anti-s-triazine antibodies and s-triazine derivatives has been investigated. The immunoassay is carried out in an indirect test format using an optical transducer for label-free monitoring of antibody binding at an immobilized hapten. The concentration of free antibody in equilibrium with the analyte is probed in a flow-through system. This format allows simple modelling of the response and assessment of the affinity constant from the calibration curve. The affinity patterns of five monoclonal antibodies and a recombinant single-chain fragment with respect to five s-triazine derivatives are determined by this method. An array of three antibodies is selected and the response pattern to mixtures of three analytes determined. Measured and calculated pattern correspond in principle, but systematic deviations are observed due to the perturbation of equilibrium during detection. The correlation of the true analyte concentration and the analyte concentrations predicted from the signal pattern using the affinity constants strongly depend on the selectivity and the affinity of the antibodies.

**Keywords:** Immunoassay; Immunoprobe; s-Triazines; Antibody array; Pattern recognition

### 1. Introduction

Immunoassay is nowadays established for trace analytics in medical, food and environmental applications. Rapid and simple test schemes combined with low-cost equipment makes immunoassay an alternative to more costly instrumental analytics. Various test schemes and detection methods have been investigated [1]. In recent years direct immuno-probes allowing label-free detection of the interaction between the antibody and the target analyte have proved their capabilities as fast, simple and nevertheless highly sensitive methods. In particular, for the detection of pesticides in drinking water various applications of such transducers have been reported [2–6].

Immunoassay is based on the high affinity binding of the analyte to the binding sites of a specific antibody. The binding constant of this interaction is critical for the performance of

the immunoassay [7]. Tremendous affinities up to  $10^{10} \text{ M}^{-1}$  are observed for antibody–analyte interactions leading to detection limits in the sub-ppb range. Nevertheless, one significant drawback derives from the fundamental principle of immunoassay: antibodies show affinity to different compounds with similar molecular structure, so-called cross-reactivity. Therefore, the selectivity of this method is a limiting factor if discrimination in multianalyte systems is required. This is demonstrated in Fig. 1 for a highly selective monoclonal antibody to the triazine herbicide terbuthylazine [8]. Even in this case significant interference by the analyte atrazine, another frequently detected triazine derivative, is observed.

A straightforward approach to solving this dilemma is the application of highly selective antibodies. This approach requires extensive search, as no systematic methods for the preparation of such antibodies are available. Furthermore, antibody selectivity is limited by the induced-fit principle of the analyte–antibody interaction. A less obvious but more promising approach is to take advantage of the differences in

\* Corresponding author. Phone: +49 7071 29 74 667. Fax: +49 7071 29 6910.

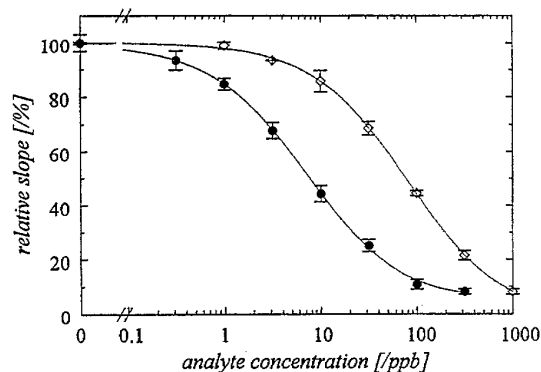


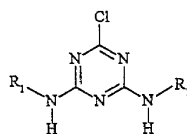
Fig. 1. Calibration curves of two analytes (atrazine and terbuthylazine) using the same antibody P6A7.

cross-reactivity usually found for antibodies by application of several antibodies with different affinity patterns. The response patterns obtained from these antibody arrays are evaluated using chemometric methods. This approach is particularly promising as techniques are established that allow variation of the affinity patterns of recombinant antibodies by site-directed mutagenesis. Arrayed transducers and microfluidics are developing as well as new concepts for microspot and multispot immunoassay allowing highly parallel multiple sample detection, which is necessary for the application of antibody arrays. In recent years, first results from multi-analyte immunoassays using antibody arrays have been investigated [9–13]. Several methods for quantitative multi-component analysis have been described using multiple regression [9] based on logistic models or model-free approaches based on neural networks [11].

Our aim is the establishment of a systematic approach to multianalyte determination by immunoassay with antibody arrays based on a test-independent parameter for the characterization of the antibody affinity pattern: the affinity constant of the analyte–antibody pair is retrieved from single analyte calibration curves [14]. The determination of antibody affinity patterns allows the selection of an effective antibody array from an antibody pool for a given analyte spectrum. Multi-analyte binding at an antibody is modelled using the affinity constants determined from the single analyte calibration. The analyte concentrations are calculated from the response pattern obtained from the antibody array. We think this approach is particularly attractive as no extensive multianalyte calibration is required for each application.

In this study we demonstrate the principle and limitations of our approach using a model system. The affinities of various monoclonal and recombinant anti-s-triazine antibodies were characterized with respect to five well-known s-triazine pesticides including one metabolite (Table 1). Calibration curves were obtained using an indirect immunoassay scheme in a flow-through system. Equilibrium free antibody concentration is determined using a rugged optical transducer, the reflectometric interference spectroscopy (RIfS), allowing

Table 1  
Structures and names of the s-triazines investigated



| Triazine         | R <sub>1</sub>                     | R <sub>2</sub>                     |
|------------------|------------------------------------|------------------------------------|
| Atrazine         | –C <sub>2</sub> H <sub>5</sub>     | –CH(CH <sub>3</sub> ) <sub>2</sub> |
| De-ethylatrazine | H                                  | –CH(CH <sub>3</sub> ) <sub>2</sub> |
| Simazine         | –C <sub>2</sub> H <sub>5</sub>     | –C <sub>2</sub> H <sub>5</sub>     |
| Propazine        | –CH(CH <sub>3</sub> ) <sub>2</sub> | –CH(CH <sub>3</sub> ) <sub>2</sub> |
| Terbuthylazine   | –C <sub>2</sub> H <sub>5</sub>     | –C(CH <sub>3</sub> ) <sub>3</sub>  |

fast detection by monitoring of antibody binding at an immobilized hapten.

An antibody array was selected for the simultaneous detection of three triazines (atrazine, propazine, terbuthylazine). Modelling of the response pattern and comparison with the measured response demonstrates the feasibility of this systematic approach. A direct calculation of analyte concentrations from the response pattern allows an estimation of the requirements and the basic limitations of multianalyte determination with antibody arrays.

### 1.1. Binding models

The heterogeneous phase immunoassay in a flow-through system described here is based on an indirect test format. Antibody is incubated with the analyte(s) and equilibrium binding to the antibody binding sites is reached. The equilibrium free antibody concentration is probed by monitoring binding at an immobilized hapten. This allows simple modelling of the response as demonstrated in detail in Ref. [15]. The signal detected as a function of analyte concentration  $c_{0,an}$  with an affinity constant  $K$  corresponds to the equilibrium concentration of antibody with free binding sites  $c_{ab,bind}$ :

$$c_{ab,bind} = \frac{c_{0,ab} - c_{0,an} - \frac{1}{K}}{2} + \sqrt{\frac{\left(c_{0,ab} + c_{0,an} + \frac{1}{K}\right)^2}{4} - c_{0,ab}c_{0,an}} \quad (1)$$

for monovalent antibody species and the concentration of antibody binding sites  $c_{0,ab}$ . A corresponding term is obtained if the distribution to the binding sites of a bivalent antibody is taken into account [15].

This expression gets far too complex for mixtures of analytes with different affinities. Simplification of the calculation is possible if

$$c_{0,ab} < K^{-1}$$

In this case the equilibrium concentration of the free analyte is very close to the initial analyte concentration, as only a minor fraction will be bound by the antibody:

$$c_{\text{an}} \approx c_{0,\text{an}}$$

The concentration of free antibody in equilibrium with analytes in the concentration  $c_{\text{an}_i}$  and the affinity constant  $K_i$  is then given by the expression

$$c_{\text{ab,bind}} = \frac{c_{0,\text{ab}}}{1 + \sum_i K_i c_{0,\text{an}_i}} \quad (2)$$

for monovalent antibody species and

$$c_{\text{ab,bind}} = c_{0,\text{ab}} \left[ \frac{1}{2} - \frac{\left( 1 - \frac{1}{1 + \sum_i K_i c_{0,\text{an}_i}} \right)^2}{2c_{0,\text{ab}}} \right] \quad (3)$$

for bivalent antibody.

Since IgG-type antibody was used for the multianalyte systems the signal patterns were calculated from the affinity constants and the analyte concentrations by using Eq. (3). Analyte concentrations were determined from the measured affinity constants by solving a linear equation system using equations of the type

$$\sum_i (K_i c_{0,\text{an}_i}) + \frac{1}{1 - \sqrt{1 - R_{\text{rel}}}} - 1 = 0 \quad (4)$$

for each antibody.

## 2. Materials and methods

### 2.1. Materials

Common chemicals and biochemicals were purchased from Sigma, Deisenhofen, Germany, and Fluka, Neu-Ulm, Germany. *s*-Triazine standard solutions in methanol (PES-TANAL™) were purchased from Riedel de Haën, Seelze, Germany. Amino dextran for surface modification was prepared according to Ref. [16]. The triazine derivative 4-chloro-6-(isopropylamino)-1,3,5-triazine-2-(6'-amino)-caproic acid (atrazine caproic acid, ACA) was a gift from Dr Ram Abukneshah, GEC London. Transducers for RIfS were manufactured by Schott, Mainz, Germany, using a plasma impulse CVD process (10 nm Ta<sub>2</sub>O<sub>5</sub> and 500 nm SiO<sub>2</sub> on float glass).

The methods for preparation of the different antibody types are published in detail elsewhere. Monoclonal antibodies were obtained by immunization of mice with hapten-BSA

conjugates and fusion of the spleen cells with myeloma cells (PAI-B<sub>3</sub>AG8) as described previously [17–19]. Recombinant scFv antibodies were obtained by a phage display method as described in Ref. [20].

### 2.2. Detection system

Reflectometric interference spectroscopy (RIfS) was used for monitoring antibody binding at a transducer surface. This technique is based on white-light interference at a thin silica layer on a glass substrate interrogated in reflected mode [21]. The experimental set-up for the detection of affinity interactions in a flow-through system was described in detail previously [22]. Recent investigations have demonstrated the capabilities of this transducer, allowing the detection of a few pg mm<sup>-2</sup> protein at the surface [23].

### 2.3. Immunoassay

The immunoassay scheme used in this study is based on the detection of the equilibrium free antibody concentration: an *s*-triazine derivative (ACA) was covalently attached in high density to a dextran matrix coupled to the surface by amide chemistry according to Ref. [16]. Inhibition of antibody binding to the surface due to binding of the analyte is detected. The test format is described in detail elsewhere [4]. After a pre-incubation of the antibody (0.5–1 μg ml<sup>-1</sup>) with the sample for at least 15 min, the sensor is exposed to this mixture. The surface is regenerated by incubation of 50 mM HCl or 2 mg ml<sup>-1</sup> pepsin at pH 1.9.

All samples were prepared in phosphate-buffered saline (PBS, 150 mM NaCl and 10 mM KH<sub>2</sub>PO<sub>4</sub>, adjusted to pH 7.4). Triazine standard solutions in various concentrations were prepared from a master solution of 1000 μg ml<sup>-1</sup>.

For the investigation of multianalyte systems, ternary mixtures of three triazines (atrazine, propazine, terbuthylazine) were prepared using a five-step 'central composite' experimental design with concentrations of each compound logarithmically equidistant between 0.32 and 31.6 ppb (17 samples). Additionally three binary mixtures and solutions containing a single analyte were taken into the matrix of samples. The analyte concentrations in these mixtures are given in Table 2.

Analyte concentrations were determined from the response pattern solving the three-dimensional equation system obtained from Eq. (4) for all three antibodies. The affinity constants determined from the single analyte calibration curve were used for the calculations.

## 3. Results and discussion

### 3.1. Affinity characterization

Inhibition of antibody binding (mab K1F4) at the transducer surface by the analyte terbuthylazine in various con-

Table 2  
Analyte concentrations in the 23 samples used for the multianalyte investigations

| No. | Atrazine (ppb) | Propazine (ppb) | Terbutylazine (ppb) |
|-----|----------------|-----------------|---------------------|
| 1   | 0.316          | 3.16            | 3.16                |
| 2   | 1              | 1               | 1                   |
| 3   | 1              | 1               | 10                  |
| 4   | 1              | 10              | 1                   |
| 5   | 1              | 10              | 10                  |
| 6   | 3.16           | 0.316           | 3.16                |
| 7   | 3.16           | 3.16            | 0.316               |
| 8   | 3.16           | 3.16            | 3.16                |
| 9   | 3.16           | 3.16            | 3.16                |
| 10  | 3.16           | 3.16            | 3.16                |
| 11  | 3.16           | 3.16            | 3.16                |
| 12  | 3.16           | 3.16            | 3.16                |
| 13  | 10             | 1               | 1                   |
| 14  | 10             | 1               | 10                  |
| 15  | 10             | 10              | 1                   |
| 16  | 10             | 10              | 10                  |
| 17  | 31.6           | 3.16            | 3.16                |
| 18  | 0              | 3.16            | 3.16                |
| 19  | 3.16           | 0               | 3.16                |
| 20  | 3.16           | 3.16            | 0                   |
| 21  | 0              | 0               | 3.16                |
| 22  | 0              | 3.16            | 0                   |
| 23  | 3.16           | 0               | 0                   |

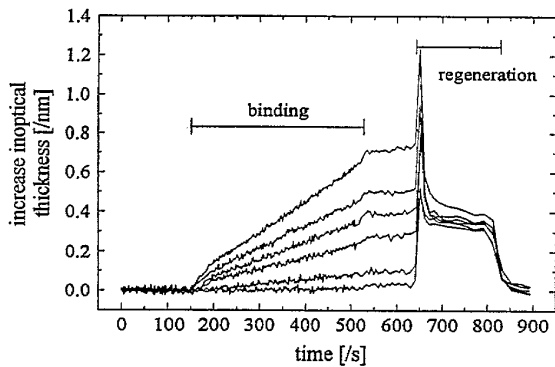


Fig. 2. Binding curves for the antibody K1F4 and terbutylazine in various concentrations. The rate of the mass-transport-limited binding is decreasing with increasing analyte concentration.

centrations (0.32–10 ppb) is demonstrated in Fig. 2. The linear binding curves are due to mass-transport-limited binding of the antibody. The slope of the curve therefore corresponds to the concentration of free antibody binding sites.

From the slope of the binding curves the calibration curve is obtained. This is shown for the same calibration in Fig. 3, including the fit of the model. An affinity constant of  $9 \times 10^8 \text{ M}^{-1}$  is obtained from the fit. In this case of a high-affinity analyte–antibody system the model corresponds well to the data points and low non-systematic residuals are observed.

A calibration curve for a low-affinity system is shown in Fig. 4 (antibody A118 with atrazine). In this case an affinity constant of  $4.4 \times 10^7 \text{ M}^{-1}$  is retrieved from the fit. Strong

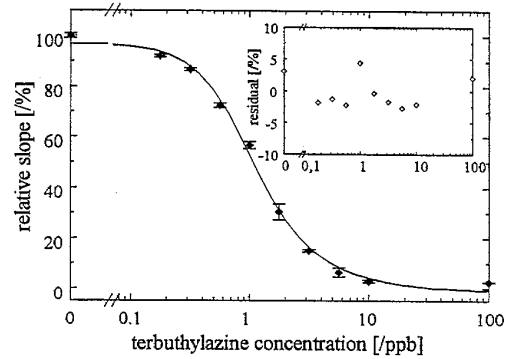


Fig. 3. Typical calibration curve for a high affinity analyte–antibody pair (K1F4 and terbutylazine,  $K = 9 \times 10^8 \text{ M}^{-1}$ ): no significant deviation of the fit from the binding model is observed.

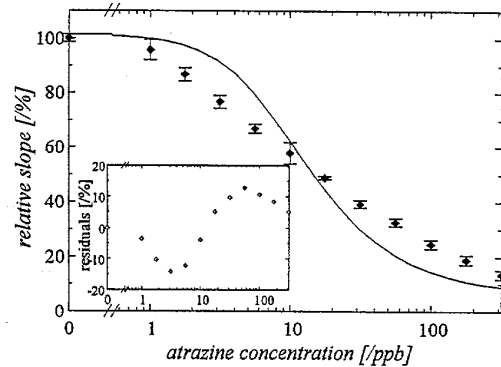


Fig. 4. Calibration of A118 with atrazine and fitting of the binding models: the residuals demonstrate significant systematic deviations.

systematic deviation from the fit is observed. This effect is due to dissociation of the hapten–antibody complex as we have discussed in more detail elsewhere [15]. For a better modelling of the calibration curve, this dissociation effect has to be taken into consideration, leading to a more complex model. As we want to demonstrate the feasibility of this approach in principle, we have started with the simple model for the description of multianalyte systems.

The affinity patterns for various monoclonal and a recombinant antibody to the five triazine analytes in focus obtained by this affinity characterization technique are shown in Fig. 5.

Affinity constants over three orders of magnitude were observed. This allows the selection of a suitable antibody array for a given analyte spectrum.

### 3.2. Multianalyte immunoassay

We have investigated the detection of ternary mixtures of atrazine, propazine and terbutylazine. Important criteria that have to be fulfilled by the selected antibody array are:

- (i) different affinity patterns for the three analytes to reach maximum analyte discrimination;
- (ii) comparable maximum affinity constants and working range.

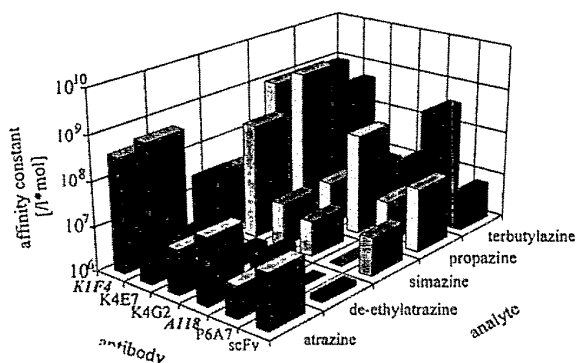


Fig. 5. Affinity patterns of various monoclonal antibodies and a recombinant scFv fragment to five selected triazines.

By these criteria the antibodies P6A7, A118 and K4G2 were chosen. The antibody P6A7 binds terbutylazine with high selectivity and the antibody A118 propazine with medium selectivity. The antibody K4G2 binds all three analytes with very similar affinity, giving a sum signal.

The responses of these three antibodies incubated with the different analyte mixtures are compared with the response modelled using Eq. (4) in Fig. 6. Good correspondence of the measured and the calculated signal is observed for the antibody P6A7. A mean deviation of 4.5% and a maximum deviation of 8% of the calculated signal from the measured signal are obtained. The antibody A118 shows a similar behaviour: a mean deviation of 4.6% and maximum deviation of 8.7% are observed. However, systematic deviations between the measured and the calculated signal are significant. This effect is even stronger for the antibody K4G2. The reason for these deviations is the same as discussed above for the single analyte calibration: dissociation of the analyte–antibody complex occurs during detection. This effect depends primarily on the dissociation rate constants of the analyte–antibody system. As the affinity of the antibody K4G2 is significantly lower than the affinity of the antibodies P6A7 and A118, more dissociation occurs due to perturbation of the equilibrium during detection.

The analyte concentrations determined from the response patterns were compared with the true concentrations for each analyte (data not shown). The mean deviations between the

Table 3

Mean absolute deviations of the predicted concentrations from the true concentrations

| Analyte concentration [ppb] | Number of samples | Deviations from true concentration [ /ppb] |           |               |
|-----------------------------|-------------------|--|-----------|---------------|
|                             |                   | Atrazine                                   | Propazine | Terbutylazine |
| 0                           | 3                 | 3.8  | 0.7       | 0.1           |
| 0.316                       | 1                 | 5.0  | 1.1       | 0.1           |
| 1                           | 4                 | 2.0  | 1.2       | 0.1           |
| 3.16                        | 10                | 3.5  | -2.2      | -0.44         |
| 10                          | 4                 | 6.4  | -5.1      | -1.3          |
| 31.6                        | 1                 | -12.3                                      | -15.7     | 0.2           |

true and the predicted concentration are summarized in Table 3 for each analyte concentration.

Again, strong differences in the quality of results are obtained: the highest discrepancy between true and predicted concentrations is observed for the analyte atrazine. A higher concentration is systematically predicted for this analyte except for the highest atrazine concentration (31.6 ppb). The correlation is significantly better for propazine. For this analyte most of the predicted concentrations are lower than the true concentrations (taking the number of samples for each concentration into account). Very good correlation of true and predicted concentration is found for the analyte terbutylazine.

The reason for this effect is closely related to the selectivity of the antibodies and the weakness of the model applied as discussed above: Each of the three antibodies is responsible for the detection of one of the analytes. As the antibody P6A7 shows high affinity to a single analyte, terbutylazine, and therefore low deviations from the model, excellent correlation is obtained. The antibody A118 detects propazine with medium affinity and stronger cross-reactivity to the other analytes. The antibody K4G2 shows low to medium affinity to all three analytes. The systematic deviation of the model is increased with decreasing affinity as discussed above, leading to an increased error in the concentration determined. Furthermore, the discrimination between the analytes atrazine and propazine becomes more critical. The determination of atrazine is the most critical as it is calculated indirectly

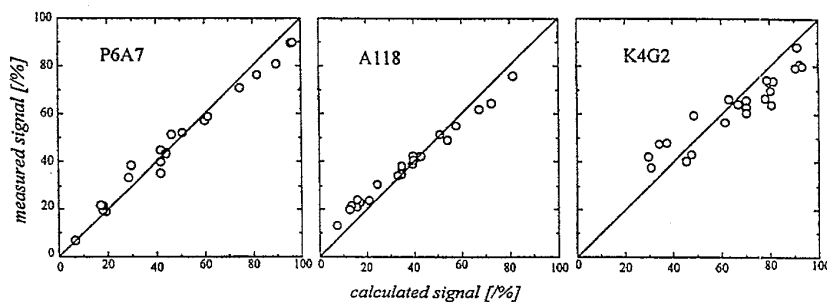


Fig. 6. Comparison of simulated and measured signals for all three antibodies.

from a sum signal of all analytes and therefore includes all errors.

#### 4. Summary and conclusions

We have investigated a model system for multianalyte detection using an antibody array with well-characterized affinity patterns. Affinity constants were derived from the calibration curves, allowing a test-independent characterization of the cross reactivities. The response patterns of a three-dimensional antibody array with different affinities and selectivities to ternary mixtures of three analytes were investigated. The signal patterns calculated from the affinity pattern corresponded well to the measured signal patterns but systematic deviations of these patterns were observed for some antibodies. They are caused by dissociation of the analyte-antibody complex during detection that are not taken into account by the model. Analyte concentrations determined from the signal patterns were compared with the true concentrations. The results obtained were of different quality corresponding to affinities of the antibodies. Improvement of the results is expected for an optimized model or an optimized antibody array.

Further development of this approach will therefore focus on an improvement of the binding model by introducing a dissociation term. Response patterns generated by a more adequate model allow detailed investigation of the capabilities and the requirements for multianalyte detection using other chemometrical methods (principal-component analysis, artificial neural networks) for the analysis of these response patterns.

#### Acknowledgements

This work was supported by the Deutsche Forschungsgesellschaft (project number Ga 235/6 1). The authors thank Dr B. Schlosshauer, NMI Reutlingen, for providing the monoclonal antibody A118.

#### References

- [1] Ch.P. Price and D.J. Newman (eds.), *Principles and Practice of Immunoassay*, Stockton Press, New York, 1991.
- [2] F.F. Bier and R.D. Schmid, Real time analysis of competitive binding using grating coupler immunosensor for pesticide detection, *Biosensors Bioelectron.*, 9 (1994) 125–130.
- [3] M. Minnuni and M. Mascini, Detection of pesticide in drinking water using real-time bio-specific interaction analysis (BIA), *Anal. Lett.*, 26 (1993) 1441–1460.
- [4] A. Brecht, J. Piehler, G. Lang and G. Gauglitz, A direct optical immunosensor for atrazine detection, *Anal. Chim. Acta*, 311 (1995) 289–299.
- [5] G. Lang, A. Brecht and G. Gauglitz, Characterisation and optimisation of an immunoprobe for triazines, *Fresenius' Z. Anal. Chem.*, 354 (1996) 857–860.
- [6] C. Mouvet, L. Almaric, S. Broussard, G. Lang, G. Brecht and G. Gauglitz, Reflectometric interference spectroscopy for the determination of atrazine in natural water samples, *Environmental Sci. Technol.*, in press (1996).
- [7] M.W. Steward and A.M. Lew, The importance of antibody affinity in the performance of immunoassays for antibody, *J. Immunol. Methods*, 78 (1985) 173–190.
- [8] T. Giersch, K. Kramer and B. Hock, Optimisation of a monoclonal antibody-based immunoassay for the detection of terbuthylazine, *Sci. Total Environment*, 132 (1993) 435–448.
- [9] M.T. Muldoon, G.F. Fries and J.O. Nelson, Evaluation of ELISA for the multianalyte analysis of s-triazines in pesticide waste and rinsate, *J. Agricult. Food. Chem.*, 41 (1993) 322–328.
- [10] P.Y.K. Cheung, L.M. Kauvar, A.E. Enquist-Goldstein and S.M. Ambler, Harnessing immunochemical cross-reactivity: use of pattern recognition to classify molecular analogs, *Anal. Chim. Acta*, 282 (1993) 181–192.
- [11] A.E. Karu, T.H. Lin, L. Breiman, M.T. Muldoon and J. Hsu, Use of multivariate statistical methods to identify immunochemical cross-reactants, *Food Agricult. Immunol.*, 6 (1994) 371–384.
- [12] M. Wortberg, S.B. Kreissig, G. Jones, D.M. Roche and B.D. Hammock, An immunoarray for the simultaneous determination of multiple triazine herbicides, *Anal. Chim. Acta*, 304 (1995) 339–352.
- [13] G. Jones, M. Wortberg, S.B. Kreissig, D.S. Bunch, S.J. Gee, B.D. Hammock and D.M. Roche, Extension of the four parameter logistic model for ELISA to multianalyte analysis, *J. Immunol. Meth.*, 177 (1994) 1–7.
- [14] J. Piehler, A. Brecht, K. Kramer, B. Hock and G. Gauglitz, Multi-analyte determination with an optical multi-antibody detection system, *Proc. SPIE*, Vol. 2504, *Environmental Monitoring and Hazardous Waste Site Remediation*, 1995, pp. 185–193.
- [15] J. Piehler, A. Brecht, Th. Giersch, B. Hock and G. Gauglitz, Assessment of affinity constants by rapid solid phase detection of equilibrium binding in a flow system, *J. Immunol. Methods*, in press.
- [16] J. Piehler, A. Brecht and G. Gauglitz, Surface modification for direct immunoprobes, *Biosensors Bioelectron.*, 11 (1996) 579–590.
- [17] T. Giersch and B. Hock, Production of monoclonal antibodies for the determination of s-triazines with enzyme immunoassay, *Food Agricult. Immunol.*, 2 (1990) 85–97.
- [18] T. Giersch, A new monoclonal antibody for sensitive detection of atrazine with immunoassay in microtiter plate and dipstick format, *J. Agricult. Food Chem.*, 41 (1993) 1006–1011.
- [19] K. Kramer, T. Giersch and B. Hock, Magnetic bead selection of hybridomas producing pesticide antibodies, *Food Agricult. Immunol.*, 6 (1994) 5–16.
- [20] K. Kramer and B. Hock, Recombinant single-chain antibodies against s-triazines, *Food Agricult. Immunol.*, 8 (1996) 97–109.
- [21] G. Gauglitz, A. Brecht, G. Kraus and W. Nahm, Chemical and biochemical sensors based on interferometry at thin (multi-)layers, *Sensors and Actuators B*, 11 (1993) 21–27.
- [22] A. Brecht and G. Gauglitz, Interferometric immunoassay in a FIA-system: a sensitive and rapid approach in label-free immunosensing, *Biosensors Bioelectron.*, 8 (1993) 387–392.
- [23] J. Piehler, A. Brecht and G. Gauglitz, Affinity detection of low molecular weight analytes, *Anal. Chem.*, 68 (1996) 139–143.